

A COMBINED MODEL FOR THE X-RAY TO γ -RAY EMISSION OF CYG X-1IGOR V. MOSKALENKO¹, WERNER COLLMAR, AND VOLKER SCHÖNFELDER

Max-Planck-Institut für extraterrestrische Physik, Postfach 1603, D-85740 Garching, Germany

ABSTRACT

We use recent data obtained by three (OSSE, BATSE, and COMPTEL) of four instruments on board the Compton Gamma Ray Observatory, to construct a model of Cyg X-1 which describes its emission in a broad energy range from soft X-rays to MeV γ -rays self-consistently. The γ -ray emission is interpreted to be the result of Comptonization, bremsstrahlung, and positron annihilation in a hot optically thin and spatially extended region surrounding the whole accretion disk. For the X-ray emission a standard corona-disk model is applied. We show that the Cyg X-1 spectrum accumulated by the CGRO instruments during a ~ 4 year time period between 1991 and 1995, as well as the HEAO-3 γ_1 and γ_2 spectra can be well represented by our model. The derived parameters match the observational results obtained from X-ray measurements.

Subject headings: elementary particles — gamma rays: theory — plasmas — radiation mechanisms: non-thermal — scattering — stars: individual (Cyg X-1)

1. INTRODUCTION

One of the brightest sources in the low-energy γ -ray sky, Cyg X-1, has been extensively studied during the last three decades since its discovery (Bowyer et al. 1965, for a review see Oda 1977, Liang & Nolan 1984). It is a high-mass binary system (HDE 226868) with an orbital period of 5.6 days consisting of a blue supergiant and presumably a black hole (BH) with a mass in excess of $5M_{\odot}$ (Dolan 1992). The separation of the two components is $\approx 4 \times 10^{12}$ cm (Beall et al. 1984). A periodicity of 294 d found in X-ray and optical light curves is thought to be related to precession of the accretion disk (Priedhorsky, Terrell, & Holt 1983, Kemp et al. 1983).

The X-ray flux of Cyg X-1 varies on all observed timescales down to a few milliseconds (e.g., Cui et al. 1997), but the average flux exhibits roughly a two-modal behaviour. Most of its time Cyg X-1 spends in a so-called ‘low’ state where the soft X-ray luminosity (2–10 keV) is low. The low-state spectrum is hard and can be described by a power-law with a photon index of ~ 1.7 in the 10–150 keV energy band. There are occasional periods of ‘high’ state emission, in which the spectrum consists of a relatively stable soft blackbody component and a weak and variable hard power-law component. Remarkable is the anticorrelation between the soft and hard X-ray components (Liang & Nolan 1984), which is clearly seen during the transition phases between the two states.

Cyg X-1 is believed to be powered by accretion through an accretion disk. Its X-ray spectrum indicates the existence of a hot X-ray emitting and a cold reflecting gas. The soft blackbody component is thought to consist of thermal emission from an optically thick and cool accretion disk (Shakura & Sunyaev 1973, Pringle 1981, Bałucińska-Church et al. 1995). The hard X-ray part ($\gtrsim 10$ keV) with a break at ~ 150 keV has been attributed to thermal emission of the accreting matter Comptonized by a hot corona with temperature from tens to hundred keV (Sunyaev & Titarchuk 1980, Liang & Nolan 1984). A broad hump peaking at ~ 20 keV (Done et al. 1992), an iron K α emission line at ~ 6.2 keV with an equivalent width ~ 100 eV (Barr, White, & Page 1985, Kitamoto et al. 1990, see

also Ebisawa et al. 1996 and references therein), and a strong iron K-edge (e.g., see Inoue 1989, Tanaka 1991, Ebisawa et al. 1992, 1996) have been interpreted as signatures of Compton reflection of hard X-rays off cold accreting material.

In addition, there have also been sporadic reports of a hard spectral component extending into the MeV region. The most famous one was the so-called ‘MeV bump’ observed at a 5σ level during the HEAO-3 mission (Ling et al. 1987). For a discussion of the pre-CGRO data and γ -ray emission mechanisms see, e.g., a review by Owens & McConnell (1992). The COMPTEL spectrum accumulated over 15 weeks of real observation time during the 1991–95 time period shows significant emission out to several MeV (McConnell et al. 1997), which, however, remained always by more than an order of magnitude below the MeV bump reported from the HEAO-3 mission.

The annihilation line search provided only tentative (1.9σ) evidence for a weak 511 keV line with a flux of $(4.4 \pm 2.4) \times 10^{-4}$ photons $\text{cm}^{-2} \text{ s}^{-1}$ (Ling & Wheaton 1989). Recent OSSE observations (Phlips et al. 1996) resulted only in upper limits with values of $\leq 7 \times 10^{-5} \text{ cm}^{-2} \text{ s}^{-1}$ for a narrow 511 keV line and $\leq 2 \times 10^{-4} \text{ cm}^{-2} \text{ s}^{-1}$ for a broad feature at 511 keV.

Although an unified view for the X-ray spectra of BH candidates and their spectral states has yet to be constructed, the qualitative picture seems to be quite clear. Current popular models include an optically thick disk component, a hot Comptonizing region (e.g., Haardt et al. 1993, Gierliński et al. 1997), and/or an advection-dominated accretion flow (e.g., Abramowicz et al. 1995, Narayan & Yi 1995 and references therein). The spectral changes are probably governed by the mass accretion rate (e.g., Chen et al. 1995, Esin, McClintock, & Narayan 1997).

This picture, however, provides no explanation for the observed γ -ray emission (e.g., McConnell et al. 1997). The hard MeV tail can not be explained by standard Compton models because they predict fluxes which are too small at MeV energies, and thus another mechanism is required. The models developed so far connect the γ -ray emission with a compact hot core (~ 400 keV or more) in the innermost part of the accretion disk,

¹and Institute for Nuclear Physics, M.V. Lomonosov Moscow State University, 119 899 Moscow, Russia

TABLE 1
LUMINOSITY OF CYG X-1.

Energy band	Luminosity, 10^{36} erg/s
≥ 0.02 MeV	26
0.02–0.2 MeV	20.5
0.2–1 MeV	4.8
≥ 1 MeV	0.6

which emits via bremsstrahlung, Compton scattering, and annihilation (Liang & Dermer 1988, Skibo & Dermer 1995), or with π^0 production due to collisions of ions with nearly virial temperature (e.g., Kolykhalov & Sunyaev 1979, Jourdain & Roques 1994). Li, Kusunose & Liang (1996) have shown that stochastic particle acceleration via wave-particle resonant interactions in plasmas (~ 100 keV) around the BH could provide a suprathermal electron population, and is able to reproduce the hard state MeV tail. The possibility of Comptonization in the relativistic gas inflow near the BH horizon has been discussed by Titarchuk & Zannias (1998).

We use the recent data obtained by three of four instruments aboard CGRO to construct a model of Cyg X-1, which describes its emission in a wide energy range from soft X-rays to MeV γ -rays (Moskalenko, Collmar, & Schönfelder 1997). Instead of a compact (pair-dominated) γ -ray emitting region, we consider an optically thin and spatially extended one surrounding the whole accretion disk. It produces γ -rays via Comptonization, bremsstrahlung and positron annihilation. For the X-ray emission the corona-disk model is retained.

In section 2 we discuss the combined OSSE–BATSE–COMPTEL spectrum of Cyg X-1. Our model and the inferred results are described in sections 3–4, and the implications are discussed in section 5. The applied formalism is given in the Appendix.

2. OBSERVATIONS

Since its launch in 1991 Cyg X-1 has been observed by CGRO several times. The time averaged COMPTEL spectrum based on all observations between the CGRO Phases 1 and 3 (April 1991 to November 1994) is shown in Fig. 1 (McConnell et al. 1997) together with the nearly contemporaneous spectrum derived from BATSE (Ling et al. 1997). The thick solid curve shows the best fit to the OSSE spectrum (0.06–1 MeV) for all observations between April 1991 and May 1995 (Phlips et al. 1996). The best-fit parameters for a power-law model with an exponential cutoff are a power-law photon index of $\Gamma = 1.39$, a cutoff energy $E_c = 158$ keV, a normalization intensity of 0.470 photons $\text{cm}^{-2} \text{ s}^{-1} \text{ MeV}^{-1}$ at 0.1 MeV. The COMPTEL data provide evidence for a hard power-law tail extending up to at least 3 MeV.

Although the OSSE and BATSE spectra have similar shapes, their intensity normalizations are different by a factor of ~ 2 (Fig. 1). The discrepancy is largest at the highest energies around 1 MeV. The COMPTEL measurements lie in between OSSE and BATSE. Although, there is no way of deducing the exact spectral shape in this region, the total spectrum is probably smooth, without bumps, which is illustrated by the three individual spectra. Possible reasons for this discrepancy have

been discussed by McConnell et al. (1997). For our further analysis we will use the combined BATSE–COMPTEL spectrum.

Table 1 lists the average luminosities of Cyg X-1 for various energy bands. The values are derived from the combined BATSE–COMPTEL spectrum assuming a source distance of 2.5 kpc. The total luminosity is between 1% and 10% of the Eddington luminosity,

$$L_{\text{Edd}} \equiv 4\pi GM \frac{m_p c}{\sigma_T} \approx 1.25 \times 10^{39} \text{ erg/s} \left(\frac{M}{10M_\odot} \right). \quad (1)$$

3. THE MODEL

The existence of a compact pair-dominated core around the BH in Cyg X-1 is unlikely in view of the CGRO observations. The signature of such a core would be a bump (Liang & Dermer 1988, Liang 1990) similar to the one reported by HEAO-3. However, no evidence for such a bump was detected by CGRO (Phlips et al. 1996, McConnell et al. 1997). In addition, the luminosity of Cyg X-1 above ~ 0.5 MeV, though small, would substantially exceed the Eddington luminosity for pairs, which is ~ 2000 times lower than that for a hydrogen plasma. On the other hand, the hard MeV tail observed by COMPTEL can not be explained by Comptonization in a corona of $kT \sim 100$ keV and therefore another mechanism is required.

Our study is an attempt to extend the ‘standard’ disk-corona model, which has been shown to work quite well at X-ray energies (e.g., Gierliński et al. 1997, Dove et al. 1997), by including the processes of γ -ray emission. We investigate the proton-dominated optically thin solution (Svensson 1984), $\Theta \equiv kT/m_e c^2 \lesssim 1$, where the γ -ray emission is attributed to a spatially extended cloud surrounding the whole accretion disk (Fig. 2), the outer corona, which emits via bremsstrahlung, Comptonization, and positron annihilation. We concentrate on the hard X-ray to γ -ray part of the spectrum, and thus we include into consideration the above-mentioned processes as well as Comptonization of the soft X-ray disk emission in the ‘standard’ inner corona. The optical depth of the outer corona has to be small enough to avoid effective reprocessing of the emission from the disk and the inner corona.

The soft X-rays consist of two components, the local blackbody emission from the disk plus the reflected spectrum. At energies above ≈ 30 keV the former is negligible and the later is only of minor importance. Therefore, we neglect both components at the moment and leave the detailed spectral modelling until the discrepancy in the intensity normalization of the OSSE and BATSE spectra has been resolved. However, the effective temperature of the soft excess is used in calculations of Comptonization in the inner and outer coronae, and the estimate of the

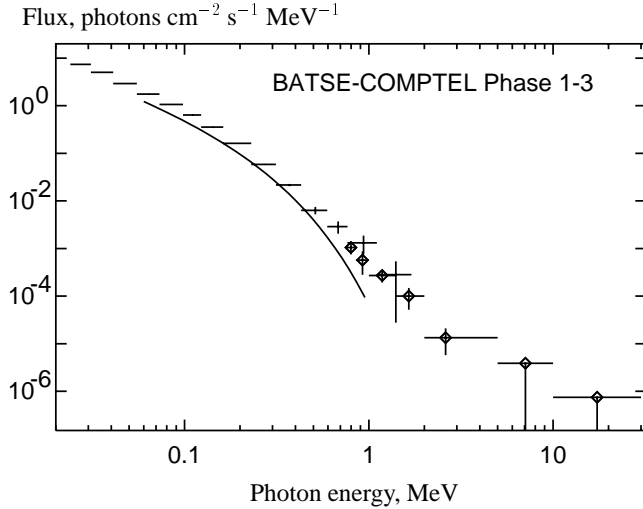


Fig. 1.— Diamonds show the average spectrum of Cyg X-1 based on all COMPTEL CGRO Phase 1–3 observations (McConnell et al. 1997) and crosses represent the almost contemporaneous BATSE data (Ling et al. 1997). The solid curve represents the best fit to the time-averaged OSSE spectrum containing 122 days of observation time. (Phlips et al. 1996).

total soft X-ray luminosity is provided to match the observed value.

Our idea is that the electrons in the outer corona (which is optically very thin) are relativistic. The heating mechanism is not specified, but people usually refer to stochastic acceleration (Li, Kusunose & Liang 1996), MHD turbulence in the inner corona (Li & Miller 1997), and plasma instabilities in magnetized advection-dominated accretion flows (Bisnovatyi-Kogan & Lovelace 1997). These mechanisms are likely to heat mainly electrons and so can provide a population of energetic particles. We further show (see Discussion) that the mean free path of these electrons in the outer corona is of the same order as its size. Because there is no mechanism to confine energetic electrons (and pairs if they exist), except for reasons of charge conservation, they can move freely inside the outer corona providing the same temperature for the whole plasma volume. Additionally, the electron cooling in a thermal plasma at low number density and small optical depth is not very efficient.

We do not consider the process of π^0 production in pp -collisions. Although it could be important at a few Schwarzschild radii (where the energy of protons is nearly virial), it is unimportant at tens to hundreds of Schwarzschild radii which is the characteristic size of the outer corona. The protons in the accreting flow far from the BH horizon should be cold, since the gravitational forces are quite weak there and thus the viscous heating in the disk is negligible. The energy transfer due to the Coulomb coupling with the hot electrons is also not efficient.

3.1. The Fitting Parameters

A set of eight fitting parameters was chosen: kT_i , τ_i , and kT_o , τ_o , the temperature and optical depth of the inner (i) and the outer (o) coronae, which are assumed to be spheres, L_{soft}^* , the luminosity of the disk which is effectively Comptonized by the inner corona, L_{soft} , the total effective soft X-ray luminosity of the central source illuminating the outer corona, R , the outer

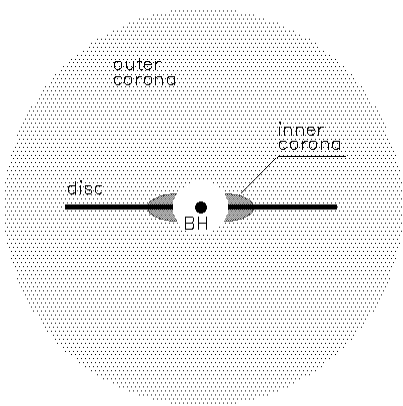


Fig. 2.— A schematic view illustrating the model.

corona radius, and, $Z = n_+/n_p$, the positron-to-proton ratio in it.

The formulae to calculate the bremsstrahlung, annihilation, and Comptonization emissivities are given in the Appendix. The accretion disk spectrum, which is further reprocessed by the inner and outer coronae, was taken to be monoenergetic with an energy $E_0 = 1.6kT_{bb}$ corresponding to the maximum of the Planck distribution, where $kT_{bb} = 0.13$ keV is the effective temperature of the soft excess (Bałucińska-Church et al. 1995).

The bremsstrahlung and annihilation photon fluxes from the outer corona are proportional to $R^3 n_i n_j$, where $n_{i,j}$ are the number densities of the plasma particles (see eqs. [A1],[A3]). Thus, if the annihilation contributes significantly, there is a continuum of solutions given by the set of equations

$$R^3 n_- n_+ \equiv R^3 n_p^2 Z(1+Z) = \frac{R \tau_o^2 Z(1+Z)}{\sigma_T^2 (1+2Z)^2} = \text{const},$$

$$\tau_o = \sigma_T R n_p (1+2Z) = \text{const}, \quad (2)$$

where kT_o is fixed, n_p is the proton number density, σ_T is the Thomson cross section, and $Z(1+Z)/(1+2Z)^2$ varies slowly for $Z \gtrsim 0.5$ (therefore, the fitting procedure is not very sensitive to this parameter). If only a negligible positron fraction is present, the continuum of solutions is defined by

$$\tau_o = R n_p \sigma_T = \text{const}, \quad (3)$$

where kT_o is fixed, $R \leq R_{\text{max}}$, and R_{max} is fixed from the fitting procedure.

4. RESULTS

The observed spectra of Cyg X-1 are shown in Figs. 3 and 4 together with our model calculations. The Comptonized spectrum from the outer corona is only shown up to 3 MeV because

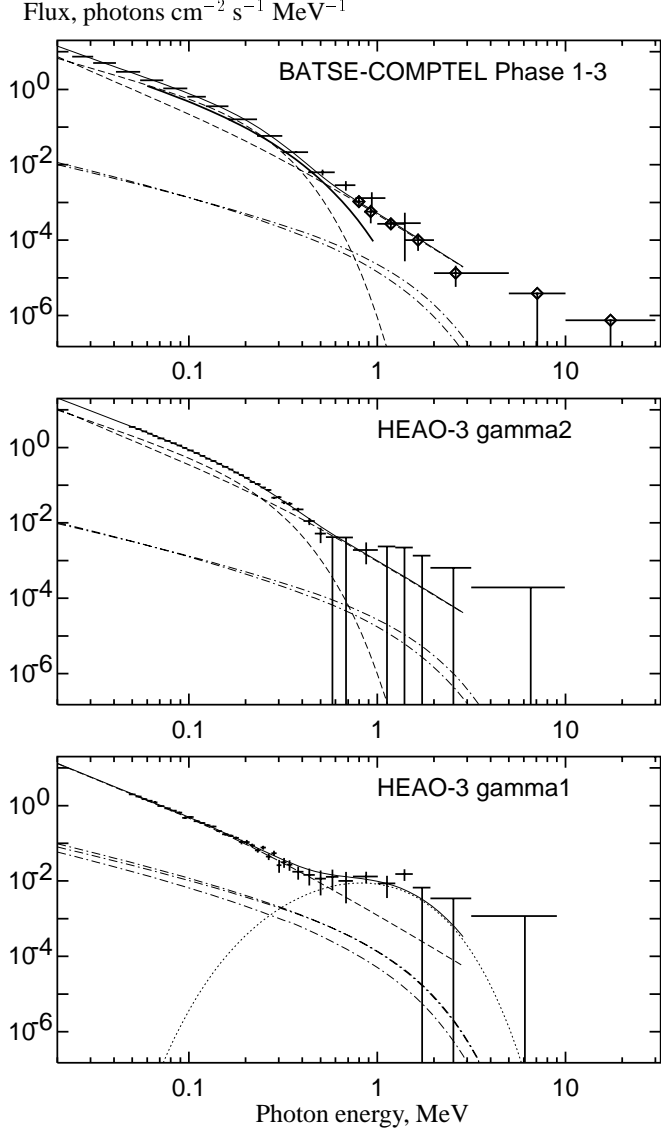


Fig. 3.— *Upper panel* shows the calculated Cyg X-1 spectrum together with the data points, which are the same as in Fig. 1. *Central and lower panels*: the HEAO-3 γ_2 , and γ_1 spectra (Ling et al. 1987). In all panels the thin solid lines represent our model fit for the parameter sets I. The individual spectral components are the annihilation line (dotted line), ee^- , e^+e^- , ep -bremsstrahlung (dash-dot), and the Comptonized spectra from the inner and outer coronae (dashed lines). The Comptonized spectra from the outer corona are shown up to 3 MeV, up to which the approximation used agrees with Monte Carlo simulations, and where also significant data points are available.

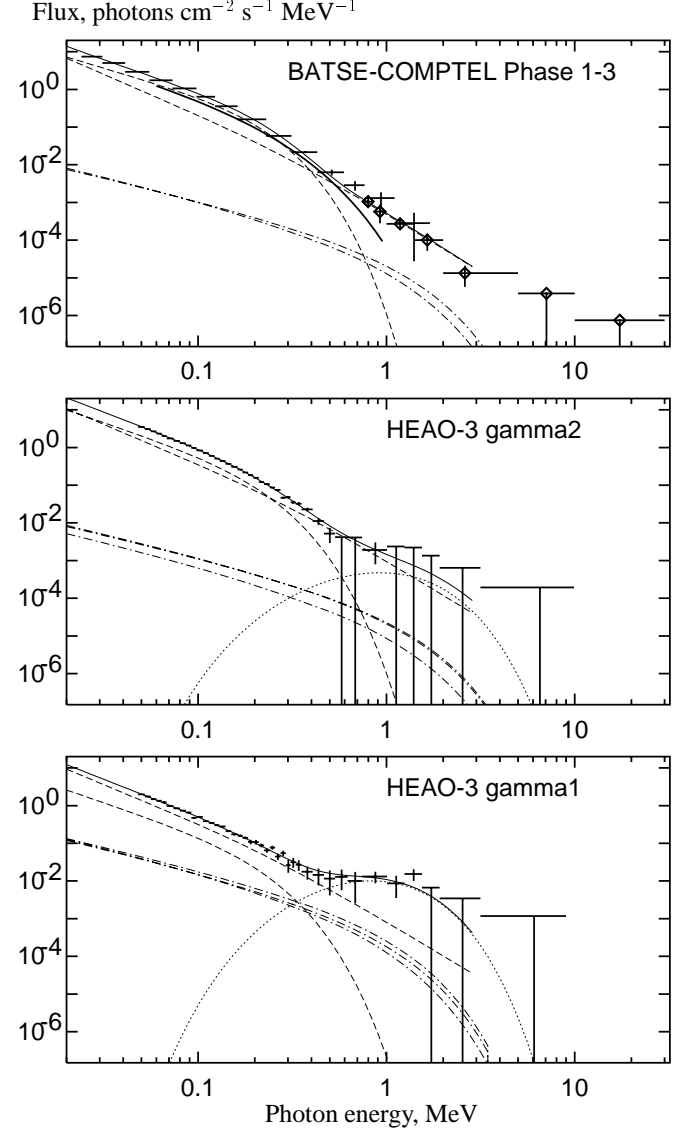


Fig. 4.— The same as in Fig. 3, but for parameter sets II (see Table 2).

TABLE 2
THE ‘BEST-FIT’ MODEL PARAMETERS.

Parameters	CGRO Phase 1–3		HEAO-3: γ_2 -state		γ_1 -state	
	I	II	I	II	I ^a	II
Soft X-ray luminosity, L_{soft} (10^{36} erg s $^{-1}$)	9.0	8.0	10.6	10.7	9.8	7.9
i -corona temperature, kT_i (keV)	76.7	79.7	95	94.9	...	93.0
i -corona optical depth, τ_i	2.39	2.23	1.41	1.42	...	1.44
L_{soft}^* , 10^{36} erg s $^{-1}$	0.73	0.84	1.96	1.95	...	0.51
o -corona temperature, kT_o (keV)	396	436	450	448	346	361
o -corona optical depth, τ_o	0.06	0.05	0.056	0.056	0.12	0.10
o -corona radius, R (10^8 cm) ^b	$\lesssim 100$	$\lesssim 100$	$\lesssim 100$	150	391	812
Positron-to-proton ratio, Z^b	0	0	0	1.0	1.0	0.5
Proton number density, n_p (10^{10} cm $^{-3}$) ^b	$\gtrsim 900$	$\gtrsim 750$	$\gtrsim 840$	187	154	93
Accretion disk radius, R_d (10^8 cm)	1	1	1
511 keV line flux, I_a (10^{-5} photons cm $^{-2}$ s $^{-1}$) ^c	0	0	0	0.18	0.15	0.04
χ^2_{ν}	4.0	3.9	1.4	1.4	0.9	0.9

^aThe inner corona is small or even absent at all

^bFor R , n_p , Z dependence see eqs. (2), (3)

^cThe narrow annihilation line flux from the disk (eq. [A4]) as calculated for the given R_d

of two reasons: the measurements above consist of upper limits only, and up to this energy our approximation (see Appendix A.2) has been tested to agree reasonably with Monte Carlo simulations. The best-fit parameters of our model are listed in Table 2. Two sets of parameters with the same χ^2_{ν} are shown² for comparison indicating that several solutions are possible. We consider the first one (I) however to be more physical.

The average BATSE–COMPTEL spectrum probably corresponds to the ‘normal’ (low) state of Cyg X-1. Only two components contribute: the Comptonized emission from the inner and outer coronae. Bremsstrahlung is of minor importance. By comparing set I and II one can see that a smaller optical depth of the outer corona corresponds to a higher temperature. The parameters obtained for the HEAO-3 γ_2 state are similar, although the spectral upper limits at high energies ($\gtrsim 1$ MeV) allow some positron fraction (set II).

The HEAO-3 γ_1 ‘bump’ spectrum has not been confirmed so far, but if true, it corresponds in our model to an outer corona size which is several times larger than in the ‘normal’ state, when the inner corona is small or even absent at all (set I). A non-negligible positron fraction (for R , n_p , Z dependence see eq. [2]) is too large to be produced in the optically thin outer corona (Svensson 1984). Therefore, we suggest a positron production mechanism (i.e., pair production in $\gamma\gamma$, γ -particle, or particle-particle collisions), which might sometimes operate in the inner disk. The radiation pressure would necessarily cause a pair wind, which serves as energy input into the outer corona thereby enlarging its radius. Note that matter outflows were found in many accreting binaries. At least two systems, 1E 1740.7–2942 and Nova Muscae, provide clear evidence for pair plasma streams (for a discussion see Moskalenko & Jour-

dain 1997a,b).

A small disk luminosity of $L_{\text{soft}}^* \approx 10^{36}$ erg/s, which is Comptonized by the *inner* corona, probably implies a geometry where only the inner part of the disk is effectively covered by the corona, which means that most of the soft X-ray photons can escape and reach the observer. The covering factor is estimated to be ~ 0.18 by applying a value of 4.7×10^{36} erg s $^{-1}$ for the total *observed* luminosity of the soft excess (Babućinska-Church et al. 1995, for a distance of 2.5 kpc). This value agrees well with a covering factor $\lesssim 0.2$ obtained by Dove et al. (1997) from self-consistent Monte Carlo modelling of the corona-disk structure. A slab (plane-parallel) corona-disk geometry is not capable to reproduce the observed broad-band X-ray spectrum of Cyg X-1 (Gierliński et al. 1997, Dove et al. 1997).

Such a picture is supported by X-ray observations. The OSSE correlation analysis of source temperature (defined from the thin thermal bremsstrahlung model) vs. 45–140 keV intensity (Phlips et al. 1996) showed that the source temperature and the intensity vary only within a limited range: $\sim 130 - 170$ keV, and $\sim 0.07 - 0.12$ photons cm $^{-2}$ s $^{-1}$, with few low-temperature – low-amplitude exceptions. A similar behaviour of the best-fit bremsstrahlung temperature vs. hard X-ray luminosity (40–200 keV) has been found by Kuznetsov et al. (1997) from the analysis of the entire dataset of the Granat/SIGMA observations of Cyg X-1 collected between 1990 and 1994.

The soft X-ray (< 10 keV) luminosity of Cyg X-1 is on the average $\sim 8.5 \times 10^{36}$ erg/s (e.g., Liang & Nolan 1984, Ebisawa et al. 1996). During the HEAO-3 γ_1 , γ_2 states it was even lower (Ling et al. 1987). Taking into account that for the hard X-ray photons the Comptonization efficiency in the hot plasma drops substantially (e.g., Hua & Titarchuk 1995) and the number of

²The value of χ^2_{ν} can not be used for the likelihood criterion estimates here mainly because of the uncertainty in the relative normalization of the OSSE, BATSE, and COMPTEL data.

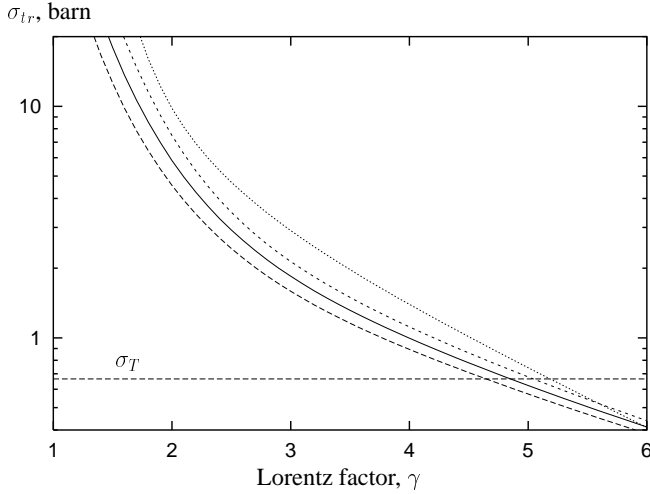


Fig. 5.— The transport cross section for electrons in a hydrogen plasma vs. the Lorentz factor of a particle. The individual lines correspond to the plasma temperatures (from top to bottom): $\Theta = 0.2, 0.6, 0.8, 1.0$. For comparison the Thomson cross section σ_T is also shown.

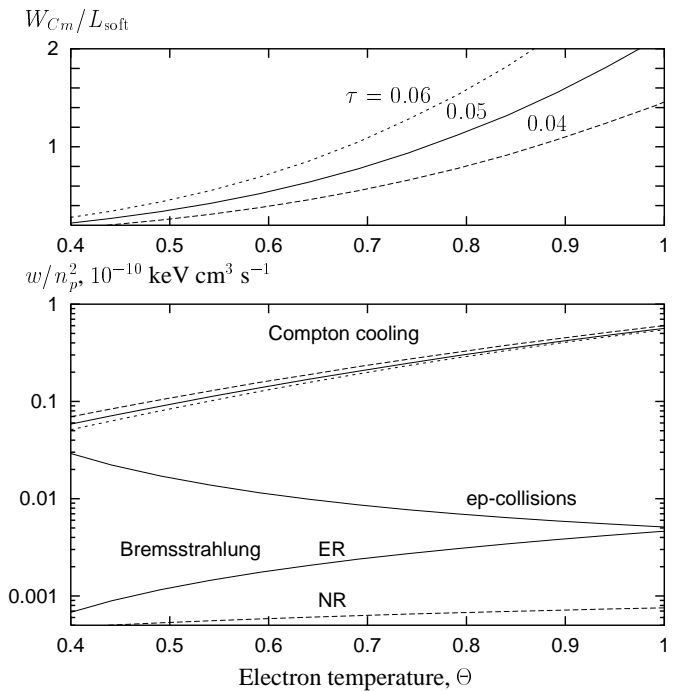


Fig. 6.— *Upper panel:* The total cooling rate due to the Compton scattering as function of the plasma temperature for several values of the optical depth (eq. B4). *Lower panel:* The cooling rates due to the electron bremsstrahlung $w_{ee} + w_{ep}$ (ER, NR) and Coulomb coupling with cold protons vs. plasma temperature ($Z = 0$, see Appendix). For the Compton scattering shown are the *average* cooling rates calculated for $R = 10^{10} \text{ cm}$, where the line styles and the optical depths correspond to these in the upper panel.

photons decreases as well, the values of $L_{\text{soft}} \approx 10^{37}$ erg/s we obtain match the observational results.

No pairs are required to reproduce the spectrum of Cyg X-1 in its normal state. If one takes an annihilation line flux of $I_a \approx 4.4 \times 10^{-4}$ photons cm $^{-2}$ s $^{-1}$ (Ling & Wheaton 1989) in the γ_1 state, the accretion disk radius is estimated to be $R_d \sim 1.7 \times 10^9$ cm (eq. [A4], set I). The upper limit allowed by optical measurements is $R_d \approx 6 \times 10^9$ cm ($M/10M_\odot$) (Liang & Nolan 1984), while the effective radius of the soft X-ray emitting region of the disk is $\sim 4.6 \times 10^7$ cm (Bafucińska-Church et al. 1995).

Our calculations show that the presented model is consistent with the available observations of the Cyg X-1 system, and is able to reproduce the observed spectra well. A more detailed study, however, would require a solution of the discrepancy in the intensity normalization between the OSSE and BATSE data and further Monte Carlo modelling.

5. DISCUSSION

We have calculated the radiation from Cyg X-1 self-consistently assuming that the hot optically thin outer corona exists. A mechanism of its maintenance was not specified in our model (so it is not *totally* self-consistent), but the energy required to maintain such a corona is quite small and could be provided by a turbulent mechanism, stochastic particle acceleration, and/or diffusion of high energy electrons from the inner disk (e.g., see Li, Kusunose & Liang 1996 and references therein). A relevant example is the solar corona of $\sim 10^6$ K (though its energetic contents is low) compared to 6000 K of the Sun's effective temperature; but a direct scaling to a BH is not appropriate here. In this section we discuss the physical conditions in the outer corona, i.e. diffusion of electrons and the cooling mechanisms, while do not touch its origin.

To treat the diffusion of energetic electrons in the outer corona we consider the *transport* cross section for *ee*-scattering. This allows us (i) to exclude unimportant scattering at small angles dominating in Coulomb interactions, and (ii) provides us with a correct estimate of the typical cross section since the *ep*-collisions in a hot plasma are of minor importance compared to *ee*-collisions.

The transport cross section σ_{tr} (see Appendix) for electrons in a hydrogen plasma of $\Theta = 0.2, 0.6, 0.8$, and 1.0 is shown in Fig. 5. Although, the value of σ_{tr} for particles with a Lorentz factor $\gamma \sim 2$ is much larger than the Thomson cross section, the corresponding mean free path of electrons is close to the radius of the outer corona. This allows electrons to pass freely and therefore provide the same temperature for the whole plasma volume. Positrons, if produced somewhere, can also homogeneously fill the plasma volume. The annihilation time scale is given by (Svensson 1982)

$$t_a = \frac{1}{\pi r_e^2 c n_-} (1 + 2\Theta^2 \ln^{-1}[1.12\Theta + 1.3]),$$

$$t_a(\Theta \sim 1) \approx 400 \text{ s} \left(\frac{10^{12} \text{ cm}^{-3}}{n_-} \right). \quad (4)$$

For the parameters listed in Table 2 t_a is of the order of hundred of seconds.

The relevant cooling rates for electrons in a pure hydrogen plasma $Z = 0$ (see Appendix) are shown in Fig. 6 (lower panel). The rates are divided by n_p^2 , the Coulomb logarithm was taken as a constant of $\ln \Lambda = 20$. For comparison we show the *average* Compton energy losses per unit volume (divided by n_p^2), $w_{Cm} n_p^{-2} = W_{Cm} n_p^{-2} \times 3/(4\pi R^3) = W_{Cm} \times 3\sigma_T^2/(4\pi R \tau_o^2)$ (see eq. [3]), calculated for $L_{\text{soft}} = 10^{37}$ erg/s, $\tau_o = 0.04, 0.05, 0.06$, and $R = 10^{10}$ cm. Clearly the *average* Comptonization losses (for τ_o fixed) depend on the radius of the outer corona and for $\Theta \gtrsim 0.4$ and the parameters adopted substantially dominate bremsstrahlung losses and losses due to the Coulomb coupling with cold protons. On the other hand, their total value is not too high, of the order of L_{soft} (upper panel), which is about 10–20% of the total luminosity.

The *average* value of the Compton energy losses of an electron in the outer corona can be estimated as $dE/dt = W_{Cm}/N$, where $N = 4\pi\tau_o R^2/3\sigma_T$ is the total number of electrons in the outer corona. Taking the corresponding numerical values (Table 2), $W_{Cm} \approx L_{\text{soft}} \sim 10^{37}$ erg/s, $\tau_o \sim 0.5$, $R = 10^{10}$ cm, one can obtain $dE/dt \approx 200$ keV/s. The appropriate timescale for an electron of $\gamma \sim 2$ is few seconds which is long compared to $R/c \lesssim 1$ sec the particle needs to cross the outer corona.

6. CONCLUSION

The data obtained recently by the CGRO instruments allow us to construct a model of Cyg X-1 which describes its emission from soft X-rays to MeV γ -rays self-consistently. This model is based on the suggestion that the γ -ray emitting region is a hot optically thin and spatially extended proton-dominated cloud, the outer corona. The emission mechanisms are bremsstrahlung, Comptonization, and positron annihilation. For X-rays a standard corona-disk model is applied.

The CGRO spectrum of Cyg X-1 accumulated over a ~ 4 years period between 1991 and 1995, as well as the HEAO-3 γ_1 , and γ_2 spectra can be well represented by our model. The derived parameters match also the basic results of the X-ray observations. A fine tuning of the model would require further Monte Carlo simulations and more accurate spectral measurements. In this respect, the solution of the discrepancy between the OSSE and BATSE normalizations would be of particular importance.

We thank the referee for useful comments. Discussions with R.Narayan, L.Titarchuk, and M.Gilfanov are greatly acknowledged. We are particularly grateful to M.McConnell for providing us with the combined spectra of Cyg X-1 prior to publication, and E.Churazov for Monte Carlo simulations of Comptonization in $\Theta \sim 1$, $\tau \approx 0.1 - 0.05$ plasma.

APPENDIX

A. RADIATION FROM A THERMAL PLASMA

For a thermal plasma consisting of electrons, positrons and protons at mildly relativistic temperatures ($kT \lesssim m_e c^2$), the main radiation processes are bremsstrahlung, electron-positron annihilation, and Compton scattering.

A.1. Bremsstrahlung

The bremsstrahlung emissivities, the number of photons emitted per unit time, per unit volume, and per unit energy interval, can be represented by the form

$$S_{ij}(\varepsilon, kT) \propto n_i n_j \frac{e^{-\varepsilon/\Theta}}{\varepsilon} G_{ij}(\varepsilon, kT), \quad (\text{A1})$$

where $\varepsilon = E/m_e c^2$ is the dimensionless photon energy, $\Theta = kT/m_e c^2$ is the dimensionless plasma temperature, and $n_{i,j}$ with $i = \{e^-, e^+\}$, $j = \{e^-, e^+, p\}$ are the corresponding number densities. Accurate numerical fits for the Gaunt factors $G_{ee}(\varepsilon, kT)$ and $G_{e^+e^-}(\varepsilon, kT)$ in an appropriate energy range have been given by Stepney & Guilbert (1983) and Haug (1987), respectively. The ep -bremsstrahlung emissivity can be calculated by the one-fold integration (e.g., see Stepney & Guilbert 1983). The approximations of the Gaunt factors $G_{ij}(\varepsilon, kT)$ have also been constructed by Skibo et al. (1995).

A.2. Comptonization

To calculate the effect of Compton scattering in a medium of $kT \sim 100$ keV we follow the model by Sunyaev & Titarchuk (1980) with corrections made by Titarchuk (1994) and Hua & Titarchuk (1995). The total number of photons emerging from the plasma cloud per unit energy interval and per unit time is given by

$$F(E, kT) = \frac{F_\nu(x, x_0)L_{\text{soft}}}{E E_0}, \quad x_0 \ll 1, \quad x_0 \ll x, \quad (\text{A2})$$

where $x \equiv E/kT$, $x_0 \equiv E_0/kT$, E is the photon energy, E_0 is the energy of soft photons injected into the plasma, L_{soft} is the luminosity of the soft photon source, and $F_\nu(x, x_0)$ is the emergent spectrum represented by the Green function (Hua & Titarchuk 1995).

The results of the Hua & Titarchuk (1995) model are generally in a good agreement with Monte Carlo simulations except at high temperatures, $\Theta \sim 1$, and small optical depth, $\tau \sim 0.1 - 0.05$ (Skibo et al. 1995). However, it still provides the correct spectral index. We found that the disagreement is mainly due to the steeper tail and the overall normalization, which is overestimated by the model. A simple power-law with an exponential cutoff, $\propto (E_0/E)^{\alpha+1}(1 - e^{-kT/E})$, where α is determined by the transcendental equation (Titarchuk & Lyubarskij 1995), gives a reasonable agreement with simulations up to ~ 3 MeV. The chosen normalization provides the correct value of the amplification factor eq. (B4).

A.3. Annihilation

The emissivity of a thermal plasma due to the electron-positron annihilation is (Dermer 1984)

$$S_a(\varepsilon, kT) = \frac{n_- n_+ c}{k T K_2^2(1/\Theta)} e^{-\frac{(2x^2+1)}{2x\Theta}} \int_1^\infty d\gamma_r (\gamma_r - 1) e^{-\frac{\gamma_r}{2x\Theta}} \sigma_a(\gamma_r), \quad (\text{A3})$$

where K_n is the modified Bessel function of the second kind and of order n , γ_r is the relative Lorentz factor of the colliding particles (invariant), and $\sigma_a(\gamma_r)$ is the annihilation cross section (Jauch & Rohrlich 1976).

The near-Earth intensity of the narrow annihilation line from the disk plane can be estimated by the assumption that all positrons which hit the disk annihilate in it (two annihilation photons per positron)

$$I_a \simeq \frac{n_+ c}{4} \frac{R_d^2}{D^2} \cos i_d, \quad (\text{A4})$$

where n_+ is the number density of positrons in the outer corona and $\frac{1}{4}n_+ c$ is the flux density toward the disk surface, R_d is the disk radius, $D = 2.5$ kpc is the distance, and i_d is the inclination angle of the disk plane ($i_d \approx 40^\circ$, Liang & Nolan 1984).

B. COOLING OF ELECTRONS

The electron cooling in a thermal plasma at low number density and small optical depth is not very effective. The main channels are: bremsstrahlung, Comptonization, and Coulomb interactions with ions (mainly protons).

B.1. Bremsstrahlung

For a pure hydrogen plasma the ep -bremsstrahlung luminosity dominates the ee -bremsstrahlung luminosity in the non-relativistic limit while at relativistic energies, $\Theta \gtrsim 0.5$, the ee -bremsstrahlung dominates. The total energy emitted per *unit volume* of plasma electrons by ep - plus e^+e^- -bremsstrahlung in the non-relativistic limit, $\Theta \ll 1$, is (Haug 1985)

$$w_{ep}^{\text{NR}} + w_{e^+e^-}^{\text{NR}} \approx \frac{128}{3\sqrt{\pi}} \alpha_f r_e^2 m_e c^3 n_p^2 \sqrt{\Theta} \left(\frac{1}{2\sqrt{2}} (1 + 2Z) + Z(1 + Z) \right), \quad (\text{B1})$$

where $\alpha_f = 1/137$ is the fine structure constant, and r_e is the classical electron radius. The total energy emitted by ee - plus e^+e^- -bremsstrahlung at the extreme-relativistic energies, $\Theta \gtrsim 1$, is given by (Alexanian 1968, Haug 1985)

$$w_{ee}^{\text{ER}} = 24\alpha_f r_e^2 m_e c^3 n_p^2 (1 + 2Z)^2 \Theta \{ \ln(2\Theta) - 0.5772 + 5/4 \}, \quad (\text{B2})$$

and that for ep -bremsstrahlung is (von Stickforth 1961, Haug 1975)

$$w_{ep}^{\text{ER}} = 12\alpha_f r_e^2 m_e c^3 n_p^2 (1 + 2Z) \Theta \{ \ln(2\Theta) - 0.5772 + 3/2 \}. \quad (\text{B3})$$

B.2. Compton cooling

An expression for the *total* energy losses of a plasma volume via Comptonization has been given by Dermer, Liang, & Canfield (1991)

$$W_{Cm} = L_{\text{soft}} \frac{P(A-1)}{1-PA} \left[1 - \left(\frac{x_0}{3} \right)^{-1-\ln P/\ln A} \right], \quad (\text{B4})$$

where

$$\begin{aligned} P &= 1 - e^{-\tau}, \\ A &= 1 + 4\Theta \frac{K_3(1/\Theta)}{K_2(1/\Theta)}, \end{aligned} \quad (\text{B5})$$

$x_0 \equiv E_0/kT$ (see eq. [A2]), and L_{soft} is the luminosity of the soft photon source. For $\tau \ll 1$ and $x_0 \ll 1$ eq. (B4) is almost exact. The luminosity enhancement factor is given by $\eta \equiv L/L_{\text{soft}} = 1 + W_{Cm}/L_{\text{soft}}$.

B.3. Coulomb Coupling with Protons

Stepney & Guilbert (1983) derived a general expression for the rate of energy transfer between populations of protons and electrons with Maxwellian distributions

$$w_{Cl} = 4 \frac{m_e}{m_p} \pi r_e^2 c n_p^2 (1 + 2Z) \ln \Lambda \frac{kT_e - kT_p}{K_2(1/\Theta_e) K_2(1/\Theta_p)} \left[2K_0 \left(\frac{\Theta_e + \Theta_p}{\Theta_e \Theta_p} \right) + \frac{2(\Theta_e + \Theta_p)^2 + 1}{\Theta_e + \Theta_p} K_1 \left(\frac{\Theta_e + \Theta_p}{\Theta_e \Theta_p} \right) \right], \quad (\text{B6})$$

where $\ln \Lambda$ is the Coulomb logarithm, $\Theta_e = kT_e/m_e c^2$, and $\Theta_p = kT_p/m_p c^2$ are the dimensionless electron and proton temperatures. The expression is symmetrical with respect to the electron and proton temperatures. In the limit of cold protons, $\Theta_p \rightarrow 0$, eq. (B6) reduces to

$$w_{Cl} = 4 \frac{m_e^2}{m_p} \pi r_e^2 c^3 n_p^2 (1 + 2Z) \ln \Lambda \frac{2\Theta_e^2 + 2\Theta_e + 1}{K_2(1/\Theta_e)}. \quad (\text{B7})$$

C. TRANSPORT CROSS SECTION

Scattering at very small angles dominates in the Coulomb cross section, which reflects the long-range nature of the Coulomb interaction. However, for the diffusion process in plasma, small scattering angles are not very important. Additionally the ep -collisions are of minor importance compared to ee -collisions. We therefore restrict ourselves by considering the transport cross section only for ee -scattering, which provides us with an estimate on typical values of the relevant cross sections.

The transport cross section for a test electron is defined by

$$\begin{aligned} \sigma_{tr}(\gamma_1) &= \int d^3 p_2 \frac{\sqrt{\gamma_r^2 - 1}}{\gamma_1 \gamma_2} f(p_2) \int d\Omega (1 - \cos \theta) \frac{d\sigma}{d\Omega} \\ &= \int d^3 p_2 \frac{\sqrt{\gamma_r^2 - 1}}{\gamma_1 \gamma_2} f(p_2) \int d\Omega^* (1 - \cos \theta) \frac{d\sigma^*}{d\Omega^*}, \end{aligned} \quad (\text{C1})$$

where β_1, γ_1 are the dimensionless speed and the Lorentz factor of the test particle, $f(p_2)$ is the Maxwell-Boltzmann distribution, $p_2 = \gamma_2 \beta_2$ is the momentum of the plasma particles, $d\sigma/d\Omega$ is the differential cross section of the Coulomb scattering (Jauch & Rohrlich 1976), and the asterisk marks the center-of-mass system (CMS) variables. The scattering angle, expressed in CMS variables, is $\cos \theta = (\beta_c + \cos \theta^*)/(1 + \beta_c \cos \theta^*)$, where $\beta_c, \gamma_c = (\gamma_1 + \gamma_2)/\sqrt{2(\gamma_r + 1)}$ are the speed and Lorentz factor of the CMS relative to the laboratory system. Changing to the integration variables γ_2 and γ_r we obtain

$$\sigma_{tr}(\gamma_1; \Theta) = \frac{1}{2\beta_1 \gamma_1^2 \Theta K_2(1/\Theta)} \int_1^\infty d\gamma_r (\gamma_r^2 - 1)^{1/2} \int_{\gamma^-}^{\gamma^+} d\gamma_2 \tilde{\sigma}_{tr}(\gamma_r, \gamma_c) e^{-\gamma_2/\Theta}, \quad (\text{C2})$$

where $\gamma^\pm = \gamma_1 \gamma_r (1 \pm \beta_1 \beta_r)$, and

$$\tilde{\sigma}_{tr}(\gamma_r, \gamma_c) = \int_{\cos \theta_M^*}^{\cos \theta_L^*} d(\cos \theta^*) \left[1 - \frac{\beta_c + \cos \theta^*}{1 + \beta_c \cos \theta^*} \right] \frac{d\sigma^*}{d(\cos \theta^*)} \quad (C3)$$

is the transport cross section for scattering angles θ^* greater than the limiting angle $\theta_L^* \rightarrow 0$, where $\theta_M^* = \pi/2$ for Møller scattering and $\theta_M^* = \pi$ for Bhabha scattering.

For Møller scattering the expression is

$$\begin{aligned} \tilde{\sigma}_{tr}(\gamma_r, \gamma_c) = & \frac{4\pi r_e^2 \gamma_r^2}{(\gamma_r - 1)^2 (\gamma_r + 1)} \left[(4\gamma_c^2 - 1) \ln \left(\frac{1 + \beta_c}{2} \right) + \frac{2(1 - \beta_c)}{1 + \beta_c} (\ln \Lambda + \ln \sqrt{2}) + 1 \right] \\ & + \frac{1}{\gamma_r + 1} \left[\left(\frac{1}{\beta_c^2} - 5 \right) \ln(1 + \beta_c) - \frac{1}{\beta_c} + 4 \ln 2 + 1 \right]. \end{aligned} \quad (C4)$$

The mean free path of a test electron in a thermal plasma would be

$$\lambda(\gamma_1; \Theta) = \frac{\beta_1}{n_- \sigma_{tr}(\gamma_1; \Theta)}. \quad (C5)$$

REFERENCES

Alexanian, M. 1968, Phys. Rev., 165, 253
 Abramowicz, M. A., et al. 1995, ApJ, 438, L37
 Bałucińska-Church, M., Belloni, T., Church, M. J., & Hasinger, G. 1995, A&A, 302, L5
 Barr, P., White, N., & Page, C. G. 1985, MNRAS, 216, 65p
 Beall, J. H., Knight, F. K., Smith, H. A., & Wood, K. S. 1984, ApJ, 284, 745
 Bisnovatyi-Kogan, G. S., & Lovelace, R. V. E. 1997, ApJ, 486, L43
 Bowyer, S., Byram, E. T., Chubb, T. A., & Friedman, M. 1965, Science, 147, 394
 Chen, X., et al. 1995, ApJ, 443, L61
 Cui, W., Zhang, S. N., Focke, W., & Swank, J. H. 1997, ApJ, 484, 383
 Dermer, C. D., Liang, E. P., & Canfield, E. 1991, ApJ, 369, 410
 Dermer, C. D. 1984, ApJ, 280, 328
 Dolan, J. F. 1992, ApJ, 384, 249
 Done, C., Mulchaey, J. S., Mushotzky, R. F., & Arnaud, K. A. 1992, ApJ, 395, 275
 Dove, J. B., Wilms, J., Maisack, M., & Begelman, M. C. 1997, ApJ, 487, 759
 Ebisawa, K., et al. 1992, Frontiers of X-Ray Astronomy, Y. Tanaka and K. Koyama (Tokyo: University Academy Press), 301
 Ebisawa, K., et al. 1996, ApJ, 467, 419
 Esin, A. A., McClintock, J. E., & Narayan, R. 1997, ApJ, 489, 867
 Gierliński, M., et al. 1997, MNRAS, 288, 958
 Haardt, F., Done, C., Matt, G., & Fabian, A. C. 1993, ApJ, 411, L95
 Haug, E. 1975, Z. Naturforsch., 30a, 1546
 Haug, E. 1985, A&A, 148, 386
 Haug, E. 1987, A&A, 178, 292
 Hua, X.-M., & Titarchuk, L. 1995, ApJ, 449, 188
 Inoue, H. 1989, 23rd ESLAB Symp. on Two Topics in X-Ray Astronomy (Noordwijk: ESA), 2, 783
 Jauch, J., & Rohrlich, F. 1976, The Theory of Photons and Electrons (New York: Springer)
 Jourdain, E., & Roques, J. P. 1994, ApJ, 426, L11
 Kemp, J. C., et al. 1983, ApJ, 271, L65
 Kitamoto, S., et al. 1990, PASJ, 42, 85
 Kolykhalov, P. I., & Sunyaev, R. A. 1979, Sov. Astron., 23, 189
 Kuznetsov S., et al. 1997, MNRAS, 292, 651
 Li, H., Kusunose, M., & Liang, E. P. 1996, ApJ, 460, L29
 Li, H., & Miller, J. A. 1997, ApJ, 478, L67
 Liang, E. P., & Dermer, C. D. 1988, ApJ, 325, L39
 Liang, E. P., & Nolan, P. L. 1984, Spa. Sci. Rev., 38, 353
 Liang, E. P. 1990, A&A, 227, 447
 Ling, J. C., Mahoney, W. A., Wheaton, Wm. A., & Jacobson, A. S. 1987, ApJ, 321, L117
 Ling, J. C., & Wheaton, Wm. A. 1989, ApJ, 343, L57
 Ling, J. C., et al. 1997, ApJS, 484, 375
 McConnell, M., et al. 1997, in AIP Conf. Proc. 410, Fourth Compton Symposium, ed. C. D. Dermer, M. S. Strickman, & J. D. Kurfess (New York: AIP), 829

Moskalenko, I. V., Collmar, W., & Schönfelder, V. 1997, in AIP Conf. Proc. 410, Fourth Compton Symposium, ed. C. D. Dermer, M. S. Strickman, & J. D. Kurfess (New York: AIP), 863 (astro-ph/9709179)

Moskalenko, I. V., & Jourdain, E. 1997a, in AIP Conf. Proc. 410, Fourth Compton Symposium, ed. C. D. Dermer, M. S. Strickman, & J. D. Kurfess (New York: AIP), 881 (astro-ph/9706283)

Moskalenko, I. V., & Jourdain, E. 1997b, *A&A*, 325, 401 (astro-ph/9702071)

Narayan, R., & Yi, I. 1995, *ApJ*, 452, 710

Oda, M. 1977, *Spa. Sci. Rev.*, 20, 757

Owens, A., & McConnell, M. L. 1992, *Comments Astrophys.*, 16, 205

Phlips, B. F., et al. 1996, *ApJ*, 465, 907

Priedhorsky, W., Terrell, J., & Holt, S. S. 1983, *ApJ*, 270, 233

Pringle, J. E. 1981, *ARA&A*, 19, 137

Shakura, N. I., & Sunyaev, R. A. 1973, *A&A*, 24, 337

Skibo, J. G., Dermer, C. D., Ramaty, R., & McKinley, J. M. 1995, *ApJ*, 446, 86

Skibo, J. G., & Dermer, C. D. 1995, *ApJ*, 455, L25

Stepney, S., & Guilbert, P. W. 1983, *MNRAS*, 204, 1269

von Stickforth, J. 1961, *Z. Physik*, 164, 1

Sunyaev, R. A., & Titarchuk, L. G. 1980, *A&A*, 86, 121

Svensson, R. 1982, *ApJ*, 258, 335

Svensson, R. 1984, *MNRAS*, 209, 175

Tanaka, Y. 1991, *Lect. Notes in Phys.* 385, Iron Line Diagnostics in X-Ray Sources, A. Treves (Berlin: Springer), 98

Titarchuk, L. G. 1994, *ApJ*, 434, 570

Titarchuk, L., & Lyubarskij, Yu. 1995, *ApJ*, 450, 876

Titarchuk, L. G., & Zannias, T. 1998, *ApJ*, 493, 863